AAPS PharmSciTech, Vol. 14, No. 3, September 2013 (© 2013)
DOI: 10.1208/s12249-013-9979-4

Research Article

Physicomechanical Characterization and Optimization of EDTA–mPEG and Avicel®–EDTA–mPEG *In Situ* Melt Dispersion Mini-Pellets

Angus R. Hibbins,[1] Yahya E. Choonara,[1] Pradeep Kumar,[1] Lisa C. du Toit,[1] and Viness Pillay[1,2]

Received 1 February 2013; accepted 8 May 2013; published online 4 June 2013

Abstract. The purpose of this study was to develop a physicomechanically customizable oral metal chelatory *in situ* hot melt dispersion mini-pellet entity which could be utilized within a binary drug delivery system. Avicel® RC/CL type R-591 was included within the *in situ* hot melt dispersion mini-pellet formulations to determine the physicomechanical effect this compound would have on the mini-pellet formulations. The physicomechanical properties of the hot melt *in situ* mini-pellet formulations were mathematically fitting to regression curves. Physicomechanical adjustment of the *in situ* hot melt dispersion mini-pellet formulations could be mathematically predicted with the derived regression curve equations. The addition of Avicel® RC/CL type R-591 increased the physicomechanical properties such as matrix hardness and increased total disintegration of the *in situ* hot melt dispersion mini-pellet formulations. The utilization of a physicomechanically customizable oral metal chelatory *in situ* hot melt dispersion mini-pellet entity within a binary drug delivery system would to achieve a synergistically enhance the activity of a drug-carrying entity or a permeation enhancing entity within a single drug delivery unit. The experimental results indicated that weights of the pellets that achieved optimal hardness ranged between 35 and 45 mg. The melt–dispersion formulations disintegrated within shorter time periods and maintained higher ethylenediaminetetraacetic acid (EDTA) concentrations whereas melt–dispersion formulations which included Avicel® had superior physicomechanical properties. Disintegration times ranged between 1,000 s for melt–dispersions containing EDTA and methyloxy polyethylene glycol 2000 (mPEG) only, to >6,000 s for melt–dispersions comprising EDTA, mPEG, and Avicel®.

KEY WORDS: chelation therapy; disintegration studies; mini-pellets; oral drug delivery; polymer melts; solid dosage forms; textual analysis.

INTRODUCTION

A binary drug delivery system is a single dosage form that contains two distinct entities and is administered as a single unit. Each distinct entity performs a unique function that will synergistically enhance the *in vivo* bioavailability of a therapeutic compound. Each entity within the drug delivery system has to be optimized in order to obtain a maximal synergistic effect. The development of an oral binary drug delivery system for drug compounds that will allow patients to avoid the parenteral route of administration will result in increased patient compliance (1–4). An example of this is the inclusion of a metal chelator containing entity and a permeation enhancer entity within a single dosage form for the oral delivery of peptide therapeutics. The metal chelator entity would exist to facilitate the accelerated libration of the metal chelator from the dosage form, before the release of the peptide therapeutic within a localized small intestine lumen environment. This study evaluates the physicomechanical properties of the *in situ* melt dispersion of ethylenediaminetetraacetic acid (EDTA) and the effect of including Avicel® RC/CL type R-591 (Avicel®) has on these *in situ* melt dispersions to facilitate the development of a predictably customizable metal chelatory containing entity.

Hot melt dispersion is a process whereby a drug entity is homogenously incorporated within a polymeric matrix without the use of solvents. This methodology requires two elements, a polymeric material that can undergo stable melting and a drug entity that is thermostable at the melting point of the polymeric material. A hot melt dispersion procedure has advantages which pertain specifically within an industrial setting. These advantages primarily rest in that a hot melt dispersion is a single-step process (polymeric material is melted at required temperature and drug mass is added to the molten polymeric material under constant aggregation) and no solvents are required which is an economical and environmental advantage (5).

A metal chelator such as EDTA has been utilized for oral delivery of peptide therapeutics because it has been indicated that EDTA decreases the localized ionic concentration load

Electronic supplementary material The online version of this article (doi:10.1208/s12249-013-9979-4) contains supplementary material, which is available to authorized users.

[1] Faculty of Health Sciences, Department of Pharmacy and Pharmacology, University of the Witwatersrand, 7 York Road, Parktown, 2193, Johannesburg, South Africa.
[2] To whom correspondence should be addressed. (e-mail: Viness.Pillay@wits.ac.za)

thereby reducing mucus viscosity and transiently reducing optimal peptidase enzyme (*i.e.*, N-aminopeptidase) activity (6–9). Additionally, EDTA has been suggested to enhance permeation of peptide therapeutics through the small intestine (7). An example of this can be reviewed in the permeation of hexarelin through the rat distal intestine that achieved an apparent permeation of 2.5 (significantly greater than sodium caprate and palmitoyl carnitine) and allowed for 91% of the peptide drug to be recovered from the rat ileum after 60 min in comparison to 55% of the peptide drug without EDTA present (10). The FDA has approved calcium disodium ethylenediaminetetraacetic acid ($CaNa_2EDTA$) for the treatment of lead poisoning (11). Methyloxy polyethylene glycol 2000 (mPEG) is known as a waxy polymer with a low melting temperature. mPEG assisted in the compactability of EDTA and enhanced the compressibility of the EDTA. Avicel® functions as a water-dispersible organic hydrocolloid that is primarily used for suspensions and emulsions. Avicel® provides an emulsion or suspension with two primary attributes, namely a structured dispersion element and a protective element (12,13). Avicel® was incorporated to determine the effect of an additional expedient to facilitate drug release. Avicel® is a spray-dried mixture of carboxymethylcellose and microcrystalline cellulose (12,13).

The EDTA–mPEG *in situ* hot melt dispersion mini-pellet formulations and Avicel®–EDTA–mPEG *in situ* hot melt dispersion mini-pellet formulations were characterized to determine the physicomechanical properties of these formulations. The physicomechanical properties of each formulation was statistically analyzed using regression curve fitting to correlate the change of a physicomechanical property with that of changing excipient weight concentration in a predictable manner. A specific physicomechanical property degree within a specific formulation can be utilized to calculate, from fitted regression curves, the degree of other measured physicomechanical properties such as matrix hardness, matrix resilience, primary disintegration rate, secondary disintegration rate, or total disintegration time. This allows for predictable physicomechanical customization of *in situ* hot melt dispersion formulations for synergistic enhancement of oral binary drug delivery systems.

MATERIALS AND METHODS

Materials

EDTA was purchased from Sigma-Aldrich, mPEG 2000 was purchased from Fluka® Analytical, Avicel® RC/CL type RC-591 (co-dried blend of microcrystalline cellulose and sodium carboxymethylcellulose) was purchased from FMC, hydrochloric acid from CJ Chem, monobasic potassium phosphate, and sodium hydroxide was purchased from Merck Chemicals.

Methods

Synthesis of EDTA–mPEG In Situ Hot Melt Dispersion Powder Formulations

The *in situ* hot melt dispersion powder formulations of EDTA–mPEG were synthesized at the weight concentration ratios represented in Table I. Avicel® was added to formulations 6–10 at a constant weight concentration of 33% *w*/*w*. The mPEG was first melted to 60°C by a calibrated hot plate magnetic stirrer. Once the solid mass of mPEG was melted to a liquid phase, EDTA was added to the molten mPEG. The EDTA was homogenously distributed within the molten mPEG. Once a uniform distribution was obtained, the EDTA–mPEG hot melt dispersion was removed from the hot plate magnetic stirrer and allowed to cool under constant stirring. Once the EDTA–mPEG hot melt dispersion had become a cool solid, the solid mass was place through a metal sieve with an aperture of 850 μm to form a fine powder.

Attenuated Total Reflectance-Fourier Transform Infrared Quantification of EDTA and Avicel®

Attenuated total reflectance-Fourier transform infrared (ATR-FTIR) quantification was performed on EDTA and Avicel® utilizing a Perkin Elmer Spectrum 2000 FTIR spectrometer with a single-reflection diamond MIRTGS detector (PerkinElmer Spectrum 100, Llantrisant, Wales, UK). Samples were prepared and placed on a diamond crystal and processed by universal ATR polarization accessory for the FTIR spectrum series at a resolution of 4 cm^{-1}. The samples were subject to a pressure of 130 psi between the scanning range of 4,000–600 cm^{-1} and were scanned to obtain a signal to noise ratio of 10. Beer's Law (Eq. 1) was utilized in order to generate a quantitative analysis of the concentrations of EDTA and Avicel® which had been serial diluted within potassium bromide.

$$A = \varepsilon l c \tag{1}$$

Where A is absorbance, ε is absorptivity, l is path length, and c is concentration.

A serial dilution of EDTA and Avicel® was prepared by utilization of potassium bromide as the diluent compound. The accurately weighed EDTA and Avicel® samples were ground with potassium bromide to produce uniform white powder samples of increasing weight concentration of each respective compound. Unique wavenumber peaks for EDTA and Avicel® was determined from the obtained ATR-FTIR spectra. A corresponding absorbance at the respective unique wavenumber peak, for each serial dilution, was determined for EDTA and Avicel®. The absorbencies of unique wavenumber peaks (n=3) were plotted on a scatter plot and a linear regression curve was fitted to these scatter points. The linear regression curve gradient was utilized for the determination of the absorptivity and path length variable (Eq. 2) as a single variable. The single variable (m) and the absorbance at the unique wavenumber peak can be used within Eq. 3 to determine the concentrations of EDTA or Avicel® form a sample that contains these compounds.

$$m = \varepsilon l \tag{2}$$

Where m is gradient of calibration curve, ε absorptivity, and l is path length.

Table I. Component Concentrations (In Percent *w*/*w*) Comprising Each Formulation

Formulation Number	EDTA (% *w*/*w*)	mPEG (% *w*/*w*)	Avicel® RC/CL R-591 (% *w*/*w*)
1	10	90	0
2	20	80	0
3	30	70	0
4	40	60	0
5	50	50	0
6	6.7	60.3	33
7	13.4	53.6	33
8	20.1	46.9	33
9	26.8	40.2	33
10	33.5	33.5	33

$$C_{\text{unknown}} = \frac{A_{\text{unknown}}}{m} \tag{3}$$

Where C_{unknown} is the unknown concentration, A_{unknown} is the absorbance of unknown sample at specific peak, and m gradient calibration curve.

Determination of EDTA Loading Using Physical Separation within Deionized Water

The weight of entrapped EDTA through physical separation was determined and compared to the loaded EDTA weight within each *in situ* melt dispersion powder formulation. The *in situ* hot melt dispersion powder formulations were accurately weighed out into three allotments of 500(±0.5) mg and dissolved within deionised water for a time period of 1 h (to ensure complete removal of mPEG from the solid phase). The solution of each allotment was then separated through filtration utilizing glass filters (0.22 μm pore size) and the glass filters were placed in an oven at 40°C overnight. The amount of entrapped EDTA within each respective allotment of the *in situ* hot melt dispersion powder formulations was determined according to Eq. 4. This was used to determine the relationship between effective EDTA entrapment and the loaded EDTA concentration within each *in situ* hot melt dispersion powder formulation.

$$W_{\text{EDTA}} = W_{\text{EDTA filter}} - W_{\text{filter}} \tag{4}$$

Where W_{EDTA} is the weight of EDTA dry mass, $W_{\text{EDTA filter}}$ is the weight of the dry filter after EDTA has been retained in the filter, and W_{filter} is the weight of the dry filter before EDTA was retained within the filter.

Zetasizer Analysis of EDTA In Situ Hot Melt Dispersion

Three EDTA samples were placed in deionised water, to obtain a concentration of 5% *w*/*v*, and were shaken at 100 rpm to ensure a uniform distribution. A volume of 10 mL 5% *w*/*v* EDTA solution from each EDTA sample was withdrawn and analyzed within the zetasizer. A volume of 10 mL 5% *w*/*v* EDTA solution from each sample was withdrawn, placed through a 0.22 μm pore filter and analyzed in the zetasizer. Three 50 mg samples of the EDTA–mPEG melt dispersion (50% *w*/*w*) was placed in deionised water (to maintain comparative EDTA concentrations) and the EDTA–mPEG *in situ* melt dispersion powder formulation samples were allowed to dissolve, liberating EDTA particles as a precipitate. The EDTA–mPEG solutions from the melt dispersion samples were shaken at 100 rpm within deionzed water and analyzed in the zetasizer. This was used to determine the size of the EDTA particles within each respective sample solution.

Differential Scanning Calorimetry of EDTA–mPEG Hot Melt Dispersion/EDTA–mPEG–Avicel® Formulations

EDTA–mPEG *in situ* hot melt dispersion powder formulations and Avicel®–EDTA–mPEG *in situ* hot melt dispersion powder formulation samples ($n=3$) were subjected to differential scanning calorimetry (DSC) analysis in a similar manner as previously reported (14). Accurately weighed samples (10±0.4 mg) were placed in a 40 μL aluminum crucible pan. An open crucible system was produced by inducing a 0.2-mm hole in the lid of the aluminum crucible pan, which was then hermetically sealed. The thermal profile of each component which makes up the mini-pellets were compared with the formulation powders to determine any change in thermal properties. DSC protocols where run with a ramping temperature of 2, 5, and 10°C/min between the temperature range of 25–110°C (first run), respectively. Each sample was analyzed again at the same respective heating rate but the temperature range was extended from 25 to 270°C (second run). The heat of fusion, onset of melting, melting peak temperatures, and crystallization peak temperatures were determined for each EDTA–mPEG *in situ* hot melt dispersion powder formulations and Avicel®–EDTA–mPEG *in situ* hot melt dispersion powder formulations.

Mini-Pellet Manufacture of EDTA–mPEG In Situ Hot Melt Dispersion Powder Formulations and Avicel®–EDTA–mPEG Powder Formulations

The EDTA–mPEG *in situ* hot melt dispersion powder formulations and Avicel®–EDTA–mPEG hot *in situ* melt dispersion powder formulations were accurately weighed into predetermined weight allotments. A modified punch and die tool was utilized to produce cylindrical mini-pellets with a diameter of 4 mm under a hydraulic pressure of 3.45 MPa from each accurately weighed allotment. The length of the cylindrical mini-pellets varied depending on the amount of powders used and the compressibility of the formulation. Each mini-pellet was weighed after manufacture and any mini-pellet which had a weight difference of greater than ±0.5 mg of the original allotment weight was discarded.

Physicomechanical Properties of EDTA–mPEG *In Situ* Hot Melt Dispersion Mini-Pellet Formulations and the Avicel®–EDTA–mPEG *In Situ* Hot Melt Dispersion Mini-Pellet Formulations

The Matrix Hardness, Matrix Resilience and Deformation Energies Studies of the In Situ Hot Melt Dispersion Mini-Pellet Formulations

The EDTA–mPEG *in situ* hot melt dispersion mini-pellet formulations and the Avicel®–EDTA–mPEG *in situ* hot melt mini-pellet formulations were evaluated with respect to matrix resilience (MR), matrix hardness (MH), and deformation energy (DE). A calibrated textual analyzer (TA.XT *plus*, Stable Microsystems, Surrey, UK) fitted with a cylindrical steel probe (50 mm diameter; for MR) and a flat tip steel probe (2 mm diameter; for MH and DE) was utilized. The parameters utilized for the analysis is outlined in Table II. All studies ($n=3$) were conducted at standard operating procedures (25°C, 1 atm pressure).

MR (in percentage) was calculated by the percentage of the ratio between the area under the curve (AUC) of the peak to baseline (after the force is removed; AUC_{2-3}) and the baseline to peak (before the force is removed; AUC_{1-2}) from a force–time profile (15). MH (in Newton per millimeter), and DE (in Joules) were both determined based on force–distance profiles. In particular, MH was elucidated from the gradient between the initial force and the maximum force attained, and the DE from the AUC (15). The matrix hardness, matrix resilience, and deformation energy for each EDTA–mPEG *in situ* melt dispersion mini-pellet formulations and Avicel®–EDTA–mPEG *in situ* melt dispersion mini-pellet formulations was determined in triplicate. The obtained measurements for each *in situ* hot melt mini-pellet formulations were plotted as scatter plots and a regression curve was fitted to each set of formulations with respect to increasing mini-pellet weight.

Disintegration Studies Determined from EDTA–mPEG In Situ Hot Melt Dispersion Mini-Pellet Formulations and Avicel®–EDTA–mPEG In Situ Hot Melt Dispersion Mini-Pellet Formulations

The disintegration studies of the EDTA–mPEG *in situ* hot melt dispersion mini-pellet formulations and Avicel®–EDTA–mPEG *in situ* hot melt dispersion mini-pellet formulations were evaluated on a textual analyzer (TA.*XT plus*, Stable Microsystems). A specialty probe was attached to the textual analyzer which facilitates the capture of a disintegration profile. Water soluble glue was used to attach the mini-pellet to a probe head which magnetically attaches to the probe shaft. A reservoir of USP 26 simulated intestinal buffer (pH 6.8) is placed under the probe. The mini-pellet is lowered into the reservoir and as the mini-pellet comes in contact with a magnetic gridded base plate, the distance from the magnetic gridded base plate to the surface of the probe head is captured. As the *in situ* hot melt dispersion mini-pellet formulation disintegrates within the simulated intestinal buffer, the probe is lowered and the distance moved over time is capture as a disintegration profile.

The disintegration parameters (primary rate of disintegration, secondary rate of disintegration, and total disintegration time) for each EDTA–mPEG *in situ* melt dispersion mini-pellet formulation and Avicel®–EDTA–mPEG *in situ* hot melt dispersion mini-pellet formulation was evaluated in triplicate. The obtained data points (including standard deviations) were placed within a scatter plot and a regression curve was applied to these scatter points for each formulation with respect to increasing mini-pellet weights. The parameters utilized for textual disintegration analysis is outlined in Table III.

Scanning Electron Microscopy Imaging of EDTA–mPEG In Situ Hot Melt Dispersion Mini-Pellet Formulations and Avicel®–EDTA–mPEG In Situ Hot Melt Dispersion Mini-Pellet Formulations

Scanning electron microscopy (SEM) imaging studies were performed ($n=3$) for each *in situ* hot melt dispersion mini-pellet formulation that had a total weight of 40 mg. The surface structures at two locations were obtained per *in situ* hot melt mini-pellet formulation for comparative purposes. Each *in situ* hot melt dispersion mini-pellet formulation was mounted on a stub with silicon tape and sputtered coated with gold for 210 s. Each mini-pellet was then placed in a FEI Phenom™ Desktop Scanning Electron Microscopy (The Netherlands, Eindhoven) so that SEM images could be acquired. The first image obtained was the edge of the *in situ* mini-pellet formulation and the second image was obtained in the inner central surface of the *in situ* mini-pellet formulation.

Statistical Analysis of Obtained Data Measurements and Regression Curves

The standard deviation of each obtained data measurement ($n=3$) was determined using Microsoft® Office Excel® 2007 (Build 12.0.4518.1014, Microsoft Corporation, USA). The obtained data measurements and the standard deviations were plotted within scatter plots using SigmaPlot V11.0 (Build 11.0.0.77, Systat Software Inc., Germany). Regression curves were fitted to the scatter plots and R^2 values for each regression curve were determined using SigmaPlot V11.0. A Shapiro–Wilk test was utilized during the calculation of each regression curve to determine if obtained data measurements were normally distributed populations at an alpha level of 0.05 using SigmaPlot V11.0. In addition, a constant variance test ($P=0.05$) for each regression curve was determined to indicate if the dependent variable remains constant despite a dynamically changing value of the independent variable using SigmaPlot V11.0. The 95% confidence interval and 95% predicted confidence interval was determined for the linear regression curves in quantitative ATR-FTIR analysis and physical separation of EDTA from *in situ* melt dispersion powder formulations was obtained using SigmaPlot V11.0.

RESULTS

Determination of Entrapped EDTA from EDTA–mPEG *In Situ* Hot Melt Dispersion Powder Formulations

Quantitative ATR-FTIR was utilized to determine the concentrations of EDTA or Avicel® that had been serial diluted within potassium bromide (Fig. 1). The absorbencies

Table II. Textural Profiling Parameters Employed for Physicochemical Characterization of the EDTA–mPEG *In Situ* Hot Melt Dispersion Mini-Pellet Formulations and Avicel®–EDTA–mPEG *In Situ* Hot Melt Dispersion Mini-Pellet Formulations

Parameters	MR (%)	MH (N/mm)	DE (J)
Pre-test speed	1 mm/s	1 mm/s	1 mm/s
Test speed	0.5 mm/s	0.5 mm/s	0.5 mm/s
Post-test speed	10 mm/s	10 mm/s	10 mm/s
Trigger type	Auto	Auto	Auto
Trigger force	0.05 N	0.05 N	0.05 N
Load cell	5 Kg	5 Kg	5 Kg
Compression strain	Variable	N/A	N/A
Target mode	Strain (40%)	Distance	Distance

MR matrix resilience, *MH* matrix hardness, *DE* deformation energy

($n=3$) of EDTA and Avicel® increased as the concentration of these compounds increased within potassium bromide.

The unique wavenumber peak of EDTA and Avicel® was determined at 1,212 and 892 cm^{-1}, respectively. The determined absorbencies ($n=3$) at this wavenumber were plotted within a scatter plot and the R^2-adjusted value was determined to be 0.98 for each fitted linear regression curve. The determined absorbencies values remained within the 95% confidence interval and the 95% predicted confidence interval. The fitted linear regression curve passed the normality test Shapiro–Wilk at an alpha level of 0.05 and the constant variance test ($P=0.05$). The serial dilution of EDTA and Avicel® within potassium bromide produced highly predictable absorbances. The quantitative ATR-FTIR could not accurately predict the concentration of entrapped EDTA within the *in situ* melt dispersion powder formulations.

The entrapped weight of EDTA within the *in situ* hot melt dispersion powder formulations were determined by physically separating the EDTA from the *in situ* hot melt dispersion powder formulations (Fig. 2). The determined entrapped EDTA weights were plotted against the loaded weight concentrations of EDTA within each *in situ* hot melt dispersion powder formulation in a highly accurate predictable manner (R^2 adjusted: 0.99). In addition, the fitted linear regression curve passed the Shapiro–Wilk test at an alpha level of 0.05 and the constant variance test ($P=0.05$). Similarly to the quantitative ATR-FTIR, the scatter plot fitted within the 95% predicted confidence interval and the 95% confidence interval. The determined entrapped weight of EDTA through physical separation was determined to correspond accurately with the loaded weight of EDTA within each *in situ* hot melt dispersion powder.

Table III. Textual Parameters Settings Employed for Disintegration Characterization of the EDTA–mPEG *In Situ* Hot Melt Dispersion Mini-Pellet Formulations and Avicel®–EDTA–mPEG *In Situ* Hot Melt Dispersion Mini-Pellet Formulations

Mode	Measure Force In Compression
Option	Hold until reset
Pre-test speed	2.0 mm/s
Test speed	3.0 mm/s
Post-test speed	10.0 mm/s
Force	10 g
Trigger type	Auto-3 g
Load cell	5 Kg
Tare mode	Auto

Zetasizer Analysis of EDTA in Hot Melt Dispersion

The Polydispersion Index (PDI) of the unfiltered EDTA, 0.22 μm injection-filtered EDTA, and Formulation 5 of the *in situ* melt dispersion powder was determined in triplicate. The PDI of unfiltered EDTA, 0.22 μm injection filtered EDTA, and Formulation 5 of the *in situ* hot melt dispersion powder was determined to be 0.351 (SD, 0.012), 0.212 (SD, 0.037), and 0.4 (SD, 0.023), respectively.

Differential Scanning Calorimetry of EDTA–mPEG Hot Melt Dispersion/EDTA–mPEG–Avicel® Formulations

The heating rate of 2°C/min generally obtained the highest heat of fusion and the slower heating rate causes the sample to undergo the process of protracted melting. Interestingly, Formulation 1 which contains EDTA–mPEG (10:90) required 65.34% less heat of fusion energy that Formulation 5 which contains EDTA–mPEG (50:50). The heat of fusion energy required to induce melting in Formulation 6, EDTA–mPEG–Avicel® (6.7:60.3:33), was determined to be 66.46% less than Formulation 10, EDTA–mPEG–Avicel® (33.5:33.5:33). Formulations 1 and 5 also demonstrated similar different heat of fusion energy required to induce melting but was at a lesser degree than formulations that contained Avicel®. The onset of melting or crystallization temperature for all the formulations remained relatively constant and for the EDTA and mPEG components. Additionally, the onset of melting or crystallization temperature did not change significantly when Avicel® was included within formulations 6–10. Similarly, the peak melting or crystallization temperature remained relatively unchanged even with the addition of Avicel®. The heat of fusion, the onset of melting, or crystallization temperature and the peak melting or crystallization temperature for Formulations 5 and 10 can be reviewed in Fig. 3. The heat of fusion, onset of melting, or crystallization temperature and peak melting or crystallization temperature can be reviewed in the Electronic Supplementary Material for Formulations 1 and 6.

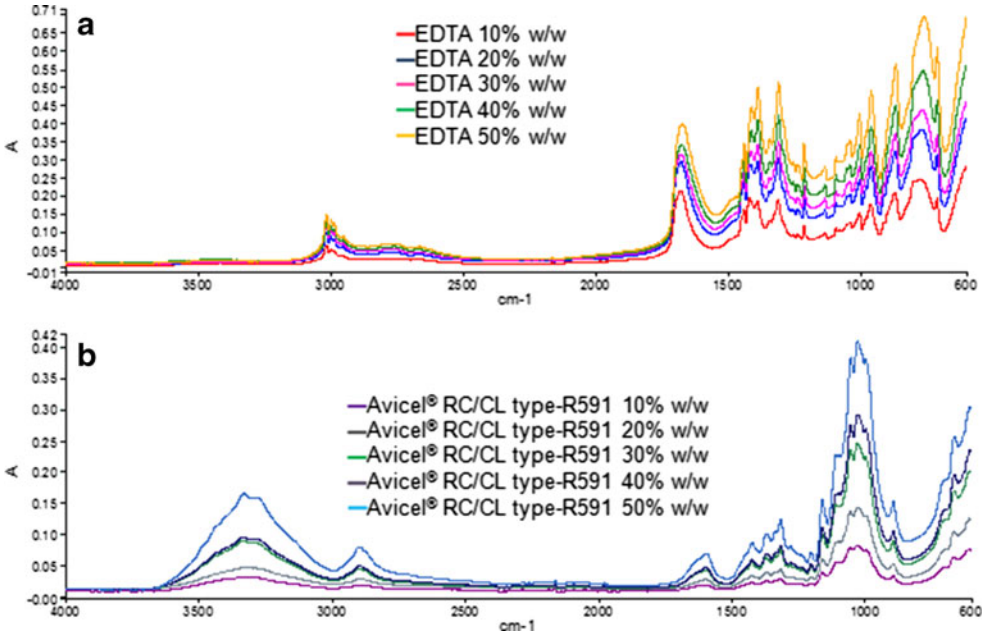

Fig. 1. ATR-FTIR spectra of different standard EDTA concentrations (**a**): 10% *w/w* (*red*), 20% *w/w* (*blue*), 30% *w/w* (*pink*), 40% *w/w* (*green*), and 50% *w/w* (*orange*) used to generate the standard curve. ATR-FTIR spectra of different standard Avicel® RC/CL type R-591 concentrations (**b**): 10% *w/w* (*light purple*), 20% *w/w* (*gray*), 30% *w/w* (*green*), 40% *w/w* (*dark purple*), and 50% *w/w* (*blue*) used to generate the standard curve. Each profile was obtained from 100 scans (SNR: 10) between a range of 4,000–600 cm^{-1} at a constant pressure of 130 psi

Physiochemical Properties of EDTA–mPEG Hot Melt Dispersion/Avicel® RC/CL Type R-591 Pellets

Matrix Hardness, Matrix Resilience, and Deformation Energies Studies

The matrix hardness, matrix resilience, and deformation energy measurement ($n=3$) for each *in situ* hot melt dispersion mini-pellet formulation was plotted within scatter plots. A regression curve was fitted to each scatter plot that achieved the highest R^2 value (between 0.94 and 1.00). The results of the EDTA–mPEG *in situ* melt dispersion mini-pellets which achieved the lowest and highest matrix hardness (Fig. 4) is represented in graphs A and B, respectively. The Avicel®–EDTA–mPEG *in situ* mini-pellets which also achieved the lowest and highest matrix hardness (Fig. 4) is represented in graphs C and D, respectively. Interestingly, the formulations which achieved the lowest matrix hardness had the least concentration of entrapped EDTA, whereas the formulations which had the highest EDTA concentration had the greatest matrix hardness. The fitted regression curve equations are represented in Fig. 5 which correlates with Fig. 4. The

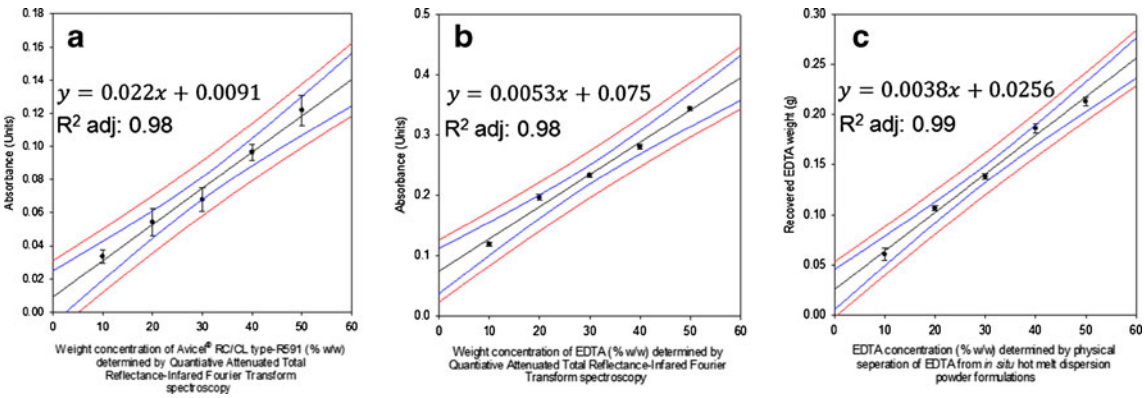

Fig. 2. Scatter plot of ethylenediaminetetraacetic acid (*red circles*) (**a**) and Avicel® RC/CL type R-591 (*blue squares*) (**b**) concentration (in percent *w/w*) against absorbance units at 1,212 and 892 cm^{-1}, respectively. Scatter plot of EDTA weight recovery (**c**) within increasing EDTA concentration (in percent *w/w*) formulations. A linear regression curve was fitted to each scatter plot and a linear regression curve fitted. Each fitted regression curve has an R^2 value, 95% confidence interval (*blue line*), 95% predicted confidence interval (*red line*) determined

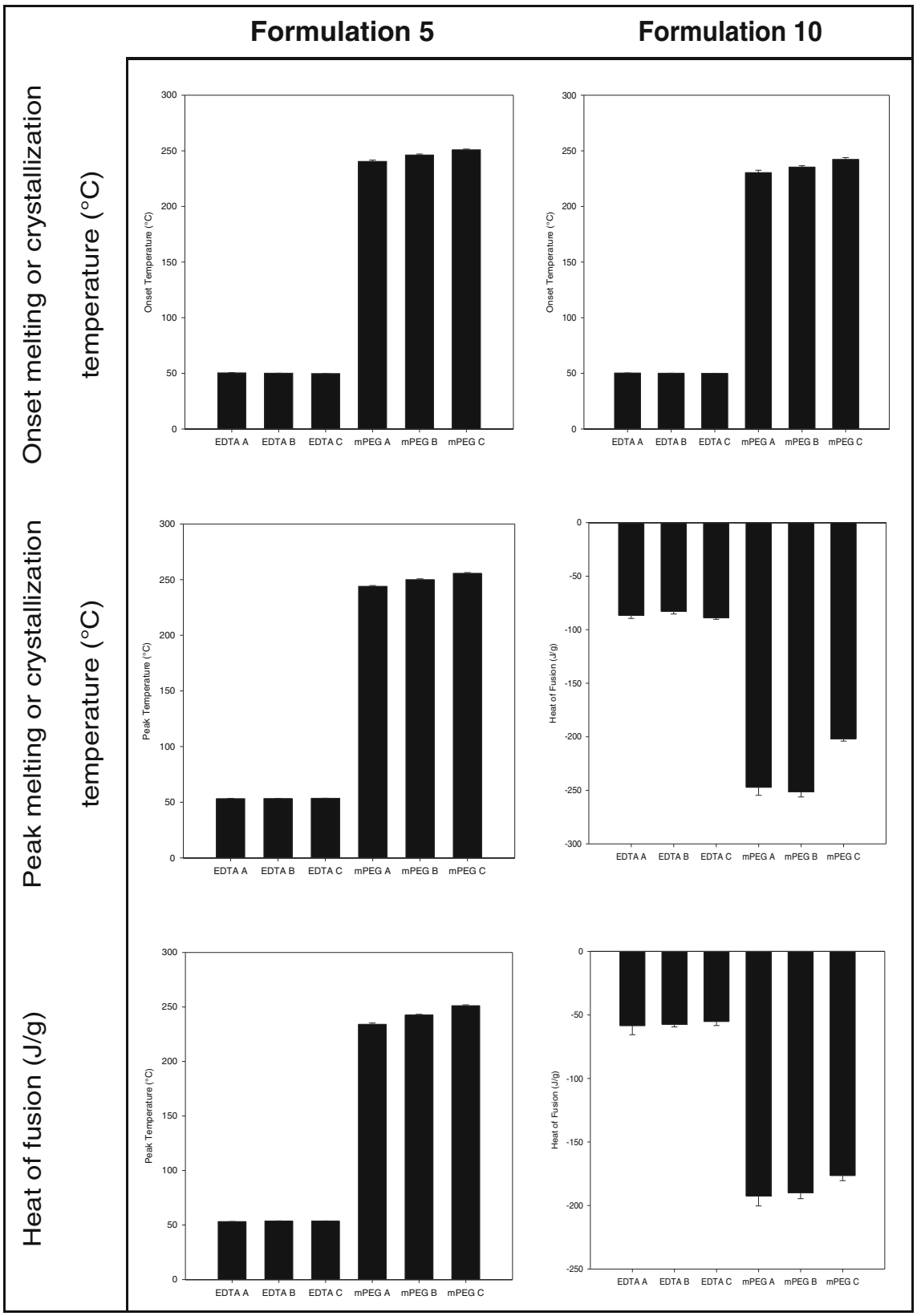

Fig. 3. Differential scanning calorimetry of Formulation 5 (EDTA–mPEG (50:50)) *in situ* hot melt dispersion powder and Formulation 10 (Avicel®–EDTA–mPEG (33:33.5:33.5)) *in situ* hot melt dispersion powder. DSC measurements determined at heating rate of 2°C are represented as A for components EDTA and mPEG. DSC measurements determined at heating rates of 5° and 10°C are represented as B and C, respectively

Shapiro–Wilk test was passed at an alpha level of 0.05 for each scatter plot and the variance constant test was passed (P=0.05) for each regression curve.

Formulation 1, which had a very low concentration of EDTA, demonstrated the least satisfactory performance in the matrix hardness evaluation. Formulation 5 which had a very high concentration of EDTA, achieved high matrix hardness. High weight concentrations of EDTA resulted in high matrix hardness which was competitive with formulations that included Avicel®.

Matrix resilience exponentially decreases as the weight of the mini-pellet for each formulation increased. The exponential decrease in matrix resilience occurred in all formulations that were assessed. The matrix resilience for formulations which contained Avicel® (Formulations 6 and 10) was less than the formulations which did not contain Avicel® (Formulations 1 and 5). Additionally, formulations which had a higher concentration of EDTA also had reduced matrix resilience. Deformation energy was determined to be constant throughout all the *in situ* melt dispersion formulations that were tested at ~0 J. The *in situ* hot melt dispersion mini-pellets were highly resistant to plastic deformation even at high-strain degrees.

EDTA–mPEG In Situ Hot Melt Dispersion Mini-Pellet and Avicel®–EDTA–mPEG In Situ Hot Melt Dispersion Mini-Pellets

The time–distance profile was analyzed and the total time of disintegration, the primary rate of disintegration, the secondary rate of disintegration, and the pellet thickness was determined by the shape of the graph (16). The measured disintegration parameters for each formulation were placed within a scatter plot. A fitted regression curve was applied to each scatter plot (Fig. 6). The determined equations of the fitted regression curve which correlates with each parameter in the respective graph can be reviewed in Fig. 7. The Shapiro–Wilk test was passed at an alpha level of 0.05 for each scatter plot and the variance constant test was passed (P=0.05) for each regression curve.

The total disintegration time increased with the increasing concentrations of EDTA within EDTA–mPEG *in situ* hot melt dispersion mini-pellets. Additionally, total disintegration time increased significantly with the addition of Avicel®. Interestingly, the primary rate of disintegration many of the *in situ* melt dispersion mini-pellet formulations plateaued or decreased with increasing mini-pellet weight. Formulation 1 pellets had the fastest disintegration time but the weakest matrix hardness whereas Formulation 10 pellets had the longest disintegration time.

Scanning Electron Microscopy Imagining of EDTA–mPEG In Situ Hot Melt Dispersion Mini-Pellet Formulation and Avicel®–EDTA–mPEG In Situ Hot Melt Dispersion Mini-Pellet Formulations

The surface structure of the *in situ* mini-pellet formulations were viewed from the edge of the *in situ* hot melt mini-pellet and the center of the *in situ* hot melt mini-pellet using SEM imaging, as seen in Fig. 8. Formulation 1, which had the highest concentration of mPEG, had the most uniform surface structure whereas Formulation 2 that had the highest concentration of EDTA has a relatively heterogeneous surface structure. Formulations 6 and 10 which contained Avicel® had microcracks in the surface structure which was not similar to those of Formulations 1 and 10.

DISCUSSION

Determination of Entrapped EDTA from EDTA–mPEG *In Situ* Hot Melt Dispersion Powder Formulations

The quantitative ATR-FTIR analysis of EDTA and Avicel® was conducted by serial dilution within potassium bromide which generated a linear standard regression curve (17). The quantitative ATR-FTIR analysis was initially utilized as a nondestructive means to determine the entrapped EDTA weight concentration within each *in situ* melt dispersion powder formulation (17). The concentration of EDTA could not be determined accurately because the mPEG had effectively coated EDTA. The ability of ATR-FTIR to detect EDTA within the mPEG melt was restricted because very little surface boundary of the EDTA molecule was exposed. An example of this is the entrapment of a drug substance within the core of cyclodextrin (18). The ability of ATR-FTIR to detect a drug substance within the cyclodextrin core is effectively reduced as the absorption and reflection of infrared light is a surface boundary phenomenon. The infrared light cannot penetrate into the cyclodextrin core or through the mPEG coating of EDTA that allows for the accurate determination of "internalized" compound concentrations. The concentration of Avicel® was difficult to determine within the *in situ* melt dispersion powder formulations because this compound is made of methyl cellulose which does not absorb strongly, relatively to EDTA and mPEG.

The loaded concentration of EDTA within *in situ* hot melt dispersion powder formulations was determined by the physical separation of EDTA from the *in situ* hot melt dispersion powder formulations. The physical separation was conducted within deionised water because EDTA that is not chelated to any metal ion species is highly insoluble within deionised water whereas mPEG is highly soluble within deionised water. The slight predictable deviation, whereby the determined weight of EDTA was higher than the original loaded mass of EDTA, is due to entrapment of mPEG within the filter. The physical separation of EDTA from the *in situ* hot melt dispersion powder formulations allowed for accurate determination of loaded EDTA.

Zetasizer Analysis of EDTA in the In Situ Hot Melt Dispersion Powder Formulations

A particle size analysis was employed since a suggested improvement of the dissolution behavior of poorly soluble active pharmaceutical ingredient (API) is facilitated when an API is placed within a solid dispersion which is partly attributed to a reduction in API particle size (19–21). This suggests that filtration of EDTA particles, through an injection filter,

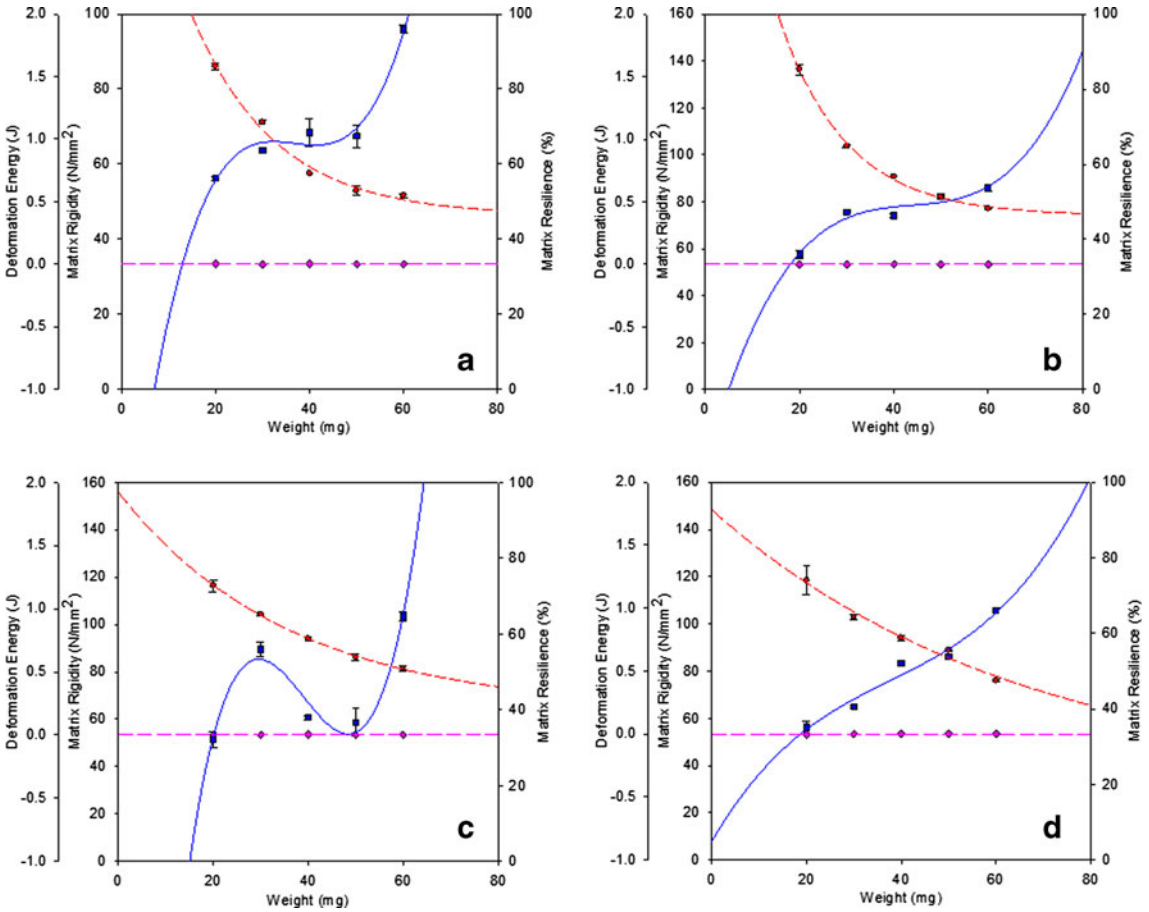

Fig. 4. The graphical representation of Formulation 1 pellets in **a** which achieved the lowest matrix hardness and the least concentration of EDTA for the melt dispersion formulations. Formulation 5 pellets in **b** achieved the greatest matrix hardness and the highest concentration of EDTA for the melt dispersion formulations. Formulation 6 pellets in **c** that achieved the lowest matrix hardness and the least concentration of EDTA for the Avicel® RC/CL type R-591 inclusive formulations. Formulation 10 pellets in **d** that achieved the greatest concentration of matrix hardness and the highest concentration of EDTA for the Avicel® RC/CL type R-591inclusive formulations. The scatter plot for matrix hardness is represented with *blue square*, the scatter plot for deformation energy is represented with *pink diamond*, the scatter plot for matrix resilience is represented with *red circle* can be reviewed in **a**–**d**. The fitted regression curve for matrix hardness is represented with *blue solid line*, the fitted regression curve for deformation energy is represented with *pink broken line*, the fitted regression curve for the matrix resilience is represented with *orange broken line* can be reviewed in **a**–**d**

forces the EDTA particles to aggregate. The EDTA–mPEG (50:50) *in situ* melt dispersion powder formulation demonstrated the smallest average particle size in comparison to filtered and unfiltered EDTA samples. Andrews *et al.* (21) and Qi *et al.* (20) may be correct that a solid dispersion of a poorly soluble API, such as EDTA, may be enhanced by a reduction in particle size. The PDI of the unfiltered EDTA was high, as expected, because there was no control over the size of particles which underwent analysis whereas the PDI of the filtered EDTA was half of that of the unfiltered EDTA. Interestingly, the EDTA–mPEG (50:50) *in situ* hot melt dispersion powder had the greatest PDI, which indicates that even though EDTA particles from this formulation had the smallest average size, there was high variability within that average size. This could be due to aggregation of EDTA within the hot melt dispersion, entropically favored, when mPEG is in the molten state but as mPEG cools, EDTA particles are effectively prevented for aggregating, hence the high PDI value.

Differential Scanning Calorimetry of EDTA–mPEG In Situ Hot Melt Dispersion Powder Formulations and Avicel®–EDTA–mPEG In Situ Hot Melt Dispersion Powder Formulations

The development of an oral pellet dosage form usually requires the homogenous mixing of dry powder excipients and drug or dissolving the powder excipients within a solvent, homogenously mixing the powder excipient solutions/suspensions with drug and then removal of the solvents takes place to generate uniform mixtures (5,22,23). The issue with mixing dry polymers within a homogenous mixture is variability that may cause slight deviations in drug concentrations within the powdered excipients but solvent mixing causes the issue with industrial waste production and some drugs degrade when exposed to solvents. Melt dispersions allow a reduction in drug loss, a more homogenous distribution with respect to drug, as well eliminating the requirement of solvents. The main issue with melt dispersions is that since the bulk phase excipient undergoes melting at a

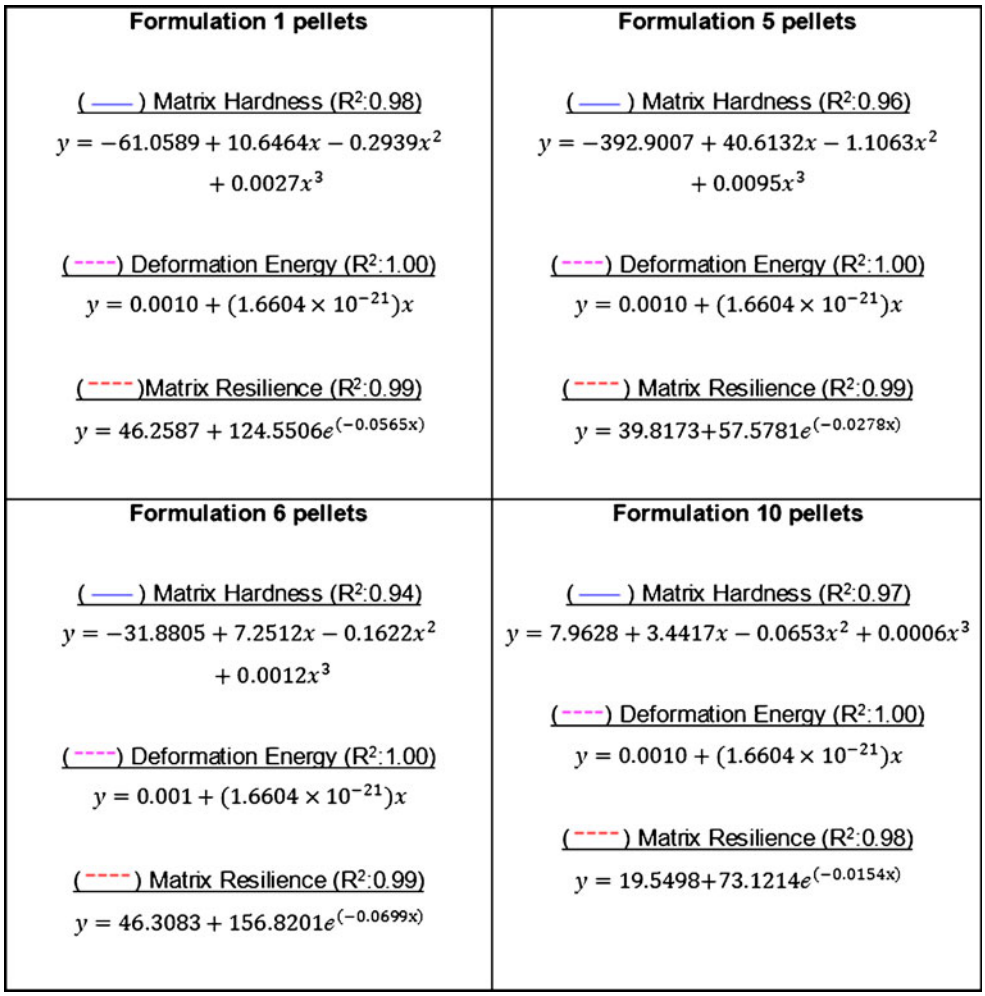

Fig. 5. The fitted regression curve equations for matrix hardness, deformation energy and matrix resilience which corresponds with **a** Formulation 1 pellets, **b** Formulation 5 pellets, **c** Formulation 6 pellets, and **d** Formulation 10 pellets

relatively low temperature, the storage life span of the final product is reduced. Additionally, if the final product experiences thermal shock (sudden increase in temperature), the drug will leach out of the melt dispersion and become unusable. The DSC of the melt dispersion formulations indicate that EDTA and mPEG formed a physical melt dispersion as the melting points for both compounds did not significantly change (24). The melting point of mPEG within these formulations was ~50°C which is above average room temperature and distribution of EDTA did not affect the heat capacity of the compound. This allows for EDTA to be released from the melt dispersion in the most potent form. In addition, Avicel®, did not alter the thermal heat capacity of EDTA or mPEG.

Physicomechanical Properties of EDTA–mPEG *In Situ* Hot Melt Dispersion Mini-Pellet Formulations and the Avicel®–EDTA–mPEG *In Situ* Hot Melt Dispersion Mini-Pellet Formulations

Matrix Hardness, Matrix Resilience, and Deformation Energies Studies

The point of indentation stresses the local intermolecular bond strength that exists between the powdered granules of the pellet by measuring the amount of force per millimeter required to indent the surface of the pellet. The greater the force required to cause an indentation within the pellet surface, the greater the bond strength between the powder granules (25). The greater the hardness, the greater amount of energy is required to break these bonds and revert a pellet back to a powder form that releases a drug (25). The matrix hardness of Formulation 1 was the least satisfactory because of the low weight concentration of EDTA and the high weight concentration of mPEG. mPEG reduces the ability of the *in situ* hot melt dispersion mini-pellet to resist localized indentation because the intermolecular bond strength the exists between mPEG polymer chains is cumulatively weak. Whereas Formulation 5 which had a high concentration of EDTA was able to achieve high matrix hardness because the localized intermolecular bonds that exist between mPEG and EDTA reinforce the macrostructure of the *in situ* hot melt dispersion mini-pellet. The inclusion of Avicel®, which is usually used within suspensions and emulsions, increases the matrix hardness of the *in situ* melt dispersion formulations because the compressibility of the formulations was enhanced. The void spaces within the macrostructure of the *in situ* minipellet formulation were effectively minimized (as seen in the disintegration studies) by the presence of Avicel®. The reduced void space volume reinforces the *in situ* mini-pellet formulation from undergoing localized indentation.

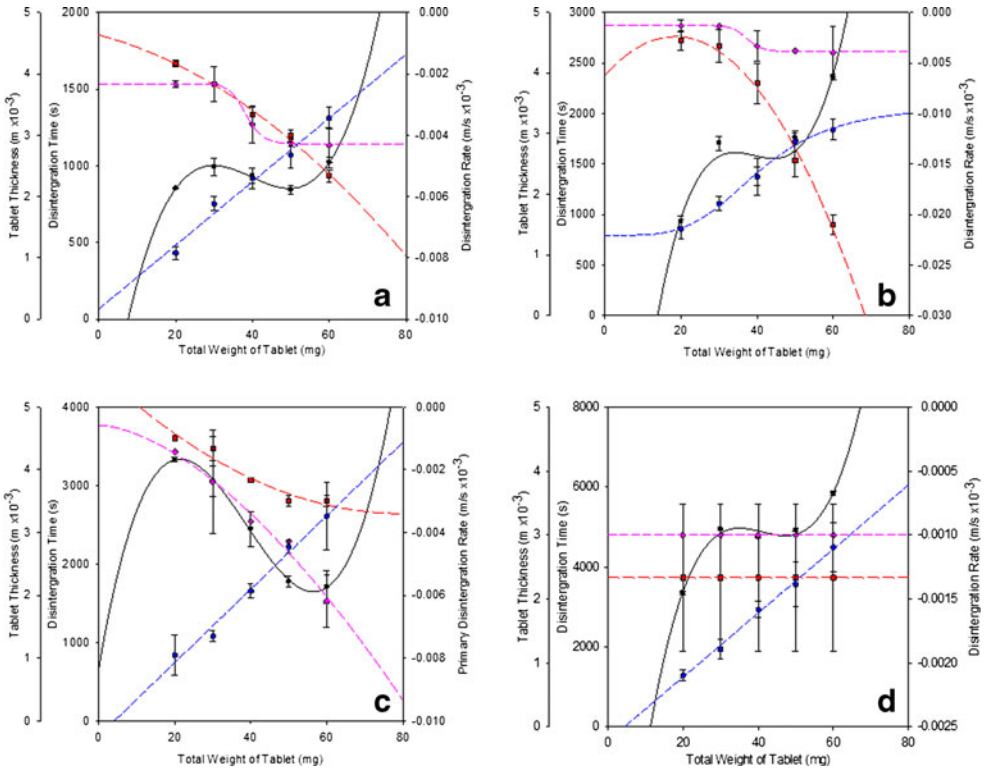

Fig. 6. The graphical representation of Formulation 1 pellets in **a** which achieved the quickest disintegration time and the least concentration of EDTA for the melt dispersion formulations. Formulation 5 pellets in **b** had the slowest disintegration time and the highest concentration of EDTA for the melt dispersion formulations. Formulation 6 pellets in **c** quickest disintegration time and the least concentration of EDTA for the Avicel® RC/CL type R-591 inclusive formulations. Formulation 10 pellets in **d** had the slowest disintegration time and the highest concentration of EDTA for the Avicel® RC/CL type R-591inclusive formulations. The scatter plot for total disintegration time is represented with *black circle*, the scatter plot for primary disintegration rate is represented with *red box*, the scatter plot for secondary disintegration rate represented with *pink diamond*, the scatter plot for pellet thickness (*blue circle*) can be reviewed in **a**–**d**. The fitted regression curve for total disintegration time is represented with *black solid line*, the fitted regression curve for primary disintegration rate is represented with *orange broken line*, the fitted regression curve for the secondary disintegration rate is represented with *pink broken line*, the fitted regression curve for pellet thickness is represented with *blue broken line* can be reviewed in **a**–**d**

The matrix resilience is the ability of a substance to deform elastically but regain form when the compressing load is removed. Within a pellet, the granules form cold wielded interfacing surfaces that have voids within the matrix of the pellet structure during the compression process within the tablet press (26). The greater the void volume within a pellet, the greater the ability of the pellet to regain form after compression until a maximal point where the strength of the intermolecular forces between the interfacing surfaces has become too weak to maintain the structure of the pellet and elastic deformation is replaced with plasticity deformation (the deformation changes the shape of the pellet permanently). Upon compression of a load onto a pellet, the intermolecular bonds are stretched. The greater the ability of the intermolecular bonds to stretch under a compressing load within a pellet, the greater the resilience of the pellet. If the compressing load becomes too great, the intermolecular bond could be broken, allowing the powder particles that comprise the pellet to form new cold-wielded interfacing surfaces, thus a permanent change in the pellet structure is forged. A hard material may have a great number of interfacing particle surfaces (physical interaction) or high strength of interfacing particle surfaces (chemical interaction) that that is so strong that a compressing load may not be enough to induce elastic deformation.

The matrix resilience in these *in situ* hot melt dispersion mini-pellet formulations decreased exponentially since the surface area of void space decreases exponentially. The *in situ* hot melt dispersion mini-pellet formulations may have high degrees of matrix hardness but a low degree of matrix resilience because the cumulative strength of the interfacing surfaces may be weak (27). This is evident in Formulation 1 which has low matrix hardness but relatively high matrix resilience, as oppose to Formulation 10 were the visa versa relationship exists.

The matrix resilience was significantly higher for formulations which had an increased amount of EDTA because greater void spaces are maintained by stronger localized bonds. The presence of Avicel® reduced matrix resilience of the *in situ* hot melt dispersion mini-pellets because the void space within the macrostructure of the mini-pellet was reduced and further compression resulted in higher Avicel® filling these void spaces to a higher degree. The physical increase in matrix hardness and reduction in matrix resilience is due to the reduced ability of the intermolecular bonds to stretch elastically into void space when a compression load is applied and assume the original bond orientation because physical matter prevents this

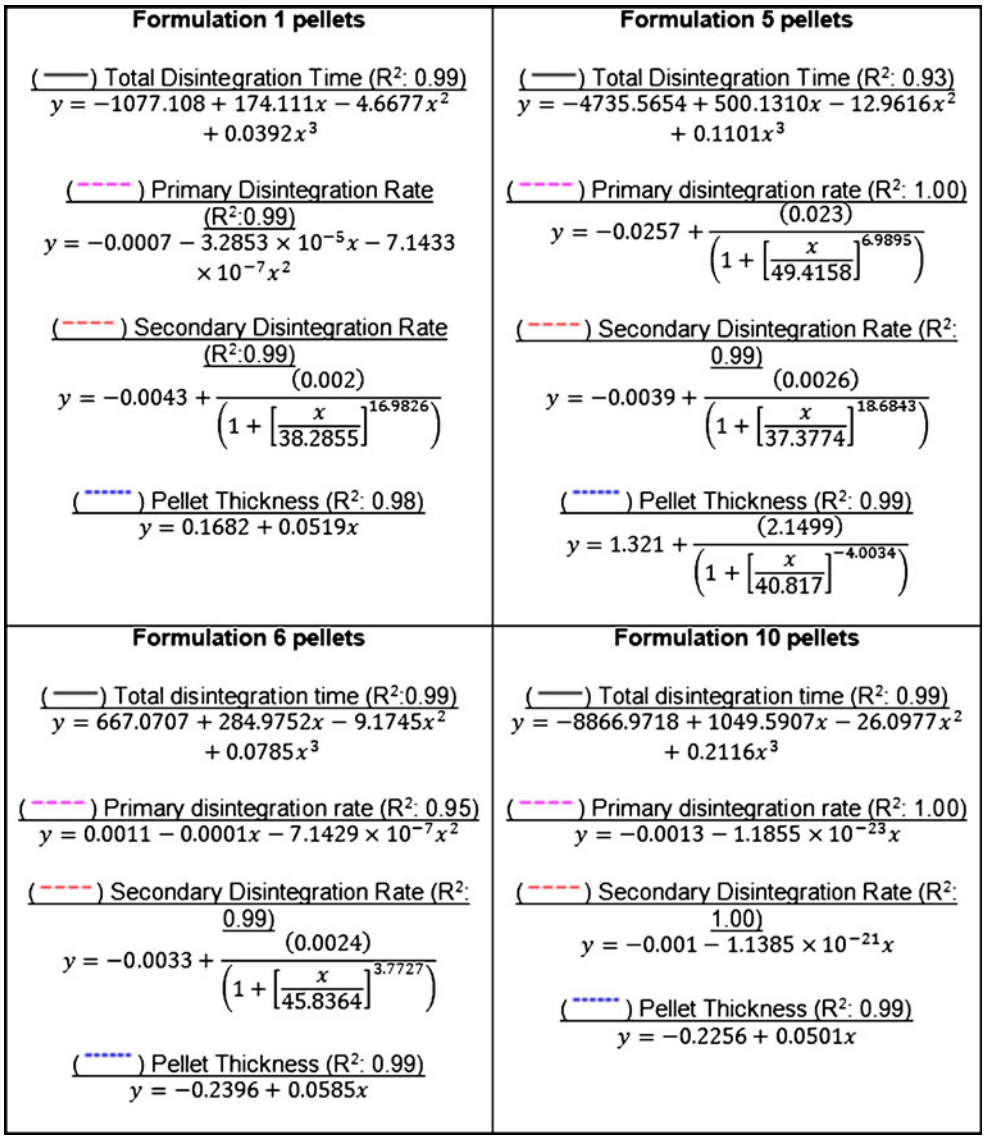

Fig. 7. The fitted regression curve equations for total disintegration time, primary rate of disintegration, secondary rate of disintegration, and pellet thickness which corresponds with **a** Formulation 1 pellets, **b** Formulation 5 pellets, **c** Formulation 6 pellets, and **d** Formulation 10 pellets

freedom of movement (28). The pellet structure internalizes the deformation energy by effectively distributing the absorbed energy throughout the structure and then dissipates the energy out of the pellet structure over time.

EDTA–mPEG In Situ Hot Melt Dispersion Mini-Pellet and Avicel®–EDTA–mPEG In Situ Hot Melt Dispersion Mini-Pellets Disintegration Studies

The total disintegration time is the required time for the pellet to loss bulk structure and the powder components which make up the pellet to become solvated within a fluid. In order for a pellet to dissolve, a solvent is needed to eliminate the strength of interfacing bonds progressively at a localized level through a mechanism of a migrating pellet surface border which moves towards the central point of the pellet. This may seem like a purely physical process whereby reduced void volume automatically increases the time required at the localized level to dissolve a pellet but this process is also highly dependent on the chemical nature of the intermolecular bond strength that forms at interfacing powder particles. If the electrostatic energy which maintains the intermolecular bonds is weak during the solvent attack on these bonds, even though there are a great number of these bonds present, the pellet would dissolve rapidly. This is due to more ineffective void elimination within the pellet structure and the increase in surface area of the pellet.

The effect that bond strength has on the total disintegration time can be observed when comparing Formulations 5 to 1. The weight concentration of EDTA within Formulation 5 was five times greater than in Formulation 5 but the total disintegration time was only 10 min longer. The intermolecular bond strength between EDTA and mPEG was strong but when the solvent had circumvented the intermolecular bond, the physical structure of the *in situ* mini-pellet disintegrated rapidly.

The primary disintegration rate is the breakdown of the *in situ* hot melt dispersion mini-pellet into granules per

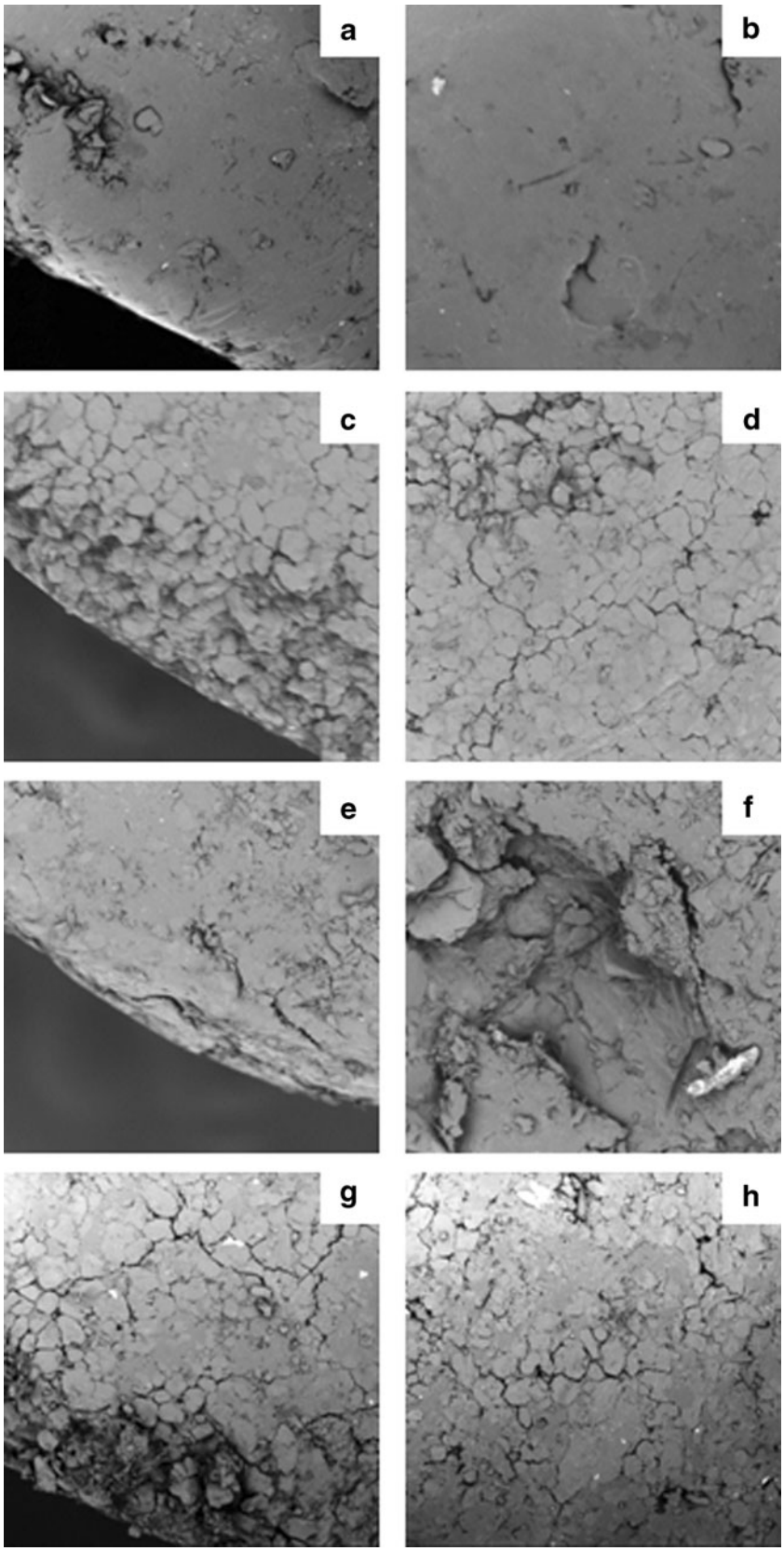

Fig. 8. Scanning electron images of the EDTA–mPEG *in situ* hot melt dispersion mini-pellet formulations and Avicel®–EDTA–mPEG *in situ* hot melt dispersion mini-pellet formulations. Images of the edge of the pellet can reviewed on the *left hand side* and the center the pellets can be reviewed on the right hand side. Formulation 1 pellet is **a** and **b**, Formulation 6 pellet is **c** and **d**, Formulation 5 pellet is **e** and **f**, Formulation 10 pellet is **g** and **h**

minute. The primary disintegration rate was determined to be the fastest in Formulation 5 pellets even though the bulk volume was the greatest whereas the primary disintegration rate was the slowest in Formulation 10. This could be due to a combination of two factors: increased surface area allows for greater localized attack of the solvent on the intermolecular bonds between particle surfaces that was formed during the cold wielding process of pellet manufacture. The presence of EDTA within mPEG induces faster primary disintegration because once the strong intermolecular bond is broken, the macrostructure of the *in situ* hot melt dispersion mini-pellet breaks down to granules very rapidly. Whereas Avicel® reduces the primary rate of disintegration because the compound effectively eliminated void spaces that resulted in reduced surface area which solvent attack may occur at cold weld spots within the macrostructure of the *in situ* hot melt dispersion mini-pellet. In combination, these compounds could be used to customize the disintegration rate of *in situ* hot melt dispersion formulations in a predictable manner.

The secondary disintegration rate is the dissolution of *in situ* hot melt dispersion mini-pellet granules. The secondary disintegration rate was determined to be the fastest when EDTA weight concentrations within *in situ* hot melt dispersion mini-pellets were at the lowest respective concentrations. This may be a benefit to the *in situ* hot melt dispersion mini-pellet formulations. For example, EDTA in these *in situ* hot melt dispersion mini-pellet formulations would benefit from a slow secondary disintegration rate as this allows the granules of these formulations to penetrate deeper into the mucosal layer and chelate divalent cations deeper within the mucosal layer (29).

The successful industrial manufacture of a solid dosage form, such as the *in situ* hot melt dispersion mini-pellets, is dependent on the degree of compressibility a formulation may achieve (29). The higher compressibility degree of a solid dosage formulation, the easier industrial manufacture of the solid dosage form can be achieved and the comfort of the patient can be increased (29). The pellet thickness directly indicates of the compressibility of the *in situ* hot melt dispersion mini-pellet formulations. For example, Formulation 10 had the greatest compressibility, but the entrapped EDTA weight concentration was not the highest of the tested formulations. Whereas Formulation 5 has the highest entrapped EDTA weight concentration but had a reduced degree of compressibility. The clinical and industrial perspective would favor Formulation 10 as opposed to Formulation 5 because Formulation 10 enhances patient comfort and will be more structurally uniform, respectively. An additional advantage of the higher compressibility of Formulation 10 is that the formulation weight could be adjusted to compensate for the reduced EDTA concentration with respect to Formulation 5 but maintain an almost equal volume. Therefore, Formulation 10 could achieve all the benefits of including Avicel® but maintains a relatively higher or similar EDTA payload to that of Formulation 5.

The Customization of EDTA–mPEG In Situ Hot Melt Dispersion Mini-Pellet Formulations and Avicel®–EDTA–mPEG In Situ Hot Melt Dispersion Mini-Pellet Formulations

The focus of this paper was determining the physicomechanical effect of Avicel® inclusion on EDTA–mPEG *is situ* hot melt dispersion mini-pellet formulations. Additionally, the predictability of physicomechanical properties effects could be accurately predicted from regression curve fitting. This allows for a customizable system to be developed where the physicomechanical properties of the formulation is predictable. An example of this is represented in Table IV. The optimal hardness with respect to *in situ* hot melt dispersion mini-pellet weight was determined from the second derivative of the fitted regression curve equation. The *in situ* hot melt dispersion mini-pellet matrix hardness, total disintegration time, primary rate of disintegration, second rate of disintegration, mini-pellet thickness and amount of loaded EDTA can be predicted from the fitted regression curves. The prediction of the physicomechanical properties of a formulation is not limited to optimal hardness but can be determined for any desired physicomechanical property.

Scanning Electron Microscopy Imagining of EDTA–mPEG In Situ Hot Melt Dispersion Mini-Pellet Formulation and Avicel®–EDTA–mPEG In Situ Hot Melt Dispersion Mini-Pellet Formulations

The surface structure of the formulation indirectly indicate the physicomechanical effect of including Avicel® and EDTA had on the macrostructure of the *in situ* hot melt dispersion mini-pellets. The SEM images of the melt dispersion formulations clearly indicate that the surface topography of EDTA–mPEG *in situ* hot melt dispersion mini-pellets is significantly more uniform than those formulations which contain Avicel®. The mPEG may have compressed at the surface level to fill large void spaces but the ability of the mPEG to fill the void space decreases within the core macrostructure of the mini-pellet.

Table IV. The Calculated Total Disintegration Time, Primary Rate of Disintegration, Secondary Rate of Disintegration and Pellet Thickness of Formulation 1 Pellets, Formulation 5 Pellets, Formulation 6 Pellets and Formulation 10 Pellets at the Optimal Hardness Weight of each Pellet Formulation. The optimal Pellet Weight, Optimal Pellet Hardness, and EDTA Weight Within for Formulations 1, 5, 6, and 10

Parameter	Formulation 1 pellets	Formulation 5 pellets	Formulation 6 pellets	Formulation 10 pellets
Weight of optimal hardness (mg)	36.284	38.8175	45.0556	36.2778
Matrix hardness (N/mm)	67.28	72.29	75.32	75.53
Total disintegration time (s)	967.717	1587.518	2062.359	4965.965
Primary rate of disintegration (mm/s)	−0.00283	−0.00629	−0.00486	−0.0013
Secondary rate of disintegration (mm/s)	−0.00287	−0.00262	−0.00206	−0.001
Pellet thickness (mm)	2.051	3.079	2.396	1.592
EDTA weight (mg)	3.63	19.41	3.02	12.15

CONCLUSIONS

The incorporation of Avicel® RC/CL type R-591 enhanced the physicomechanical properties of the *in situ* hot melt dispersion mini-pellet formulations of chelatory agent EDTA. The enhanced physicomechanical properties reduced the size of the mini-pellet macrostructure. In addition, the incorporation of Avicel® RC/CL type R-591 within the *in situ* hot melt dispersion formulation allowed for extended disintegration to occur. The physicomechanical properties, such as matrix hardness or total disintegration time, of these formulations were described using mathematical regression curve fitting. A desired physicomechanical property degree, within a specific *in situ* hot melt dispersion formulation, can mathematically predict the degree of other physicomechanical properties to create a customizable formulation for a specific application. This would be extremely useful within a binary drug delivery system where the properties of the drug-carrying entity or permeation-enhancing entity can be synergistically enhanced using a predictable customizable EDTA containing *in situ* hot melt dispersion mini-pellet formulation. The selection of the best *in situ* hot melt dispersion mini-pellet formulation could be simply selected from desired physicomechanical properties using mathematically determined regression curves to meet the needs of the binary drug delivery system.

ACKNOWLEDGMENTS

The work is funded by the National Research Fund (NRF) of South Africa.

REFERENCES

1. Makhlof A, Werle M, Tozuka Y, Takeuchi H. A mucoadhesive nanoparticulate system for the simulataneous delivery of macromolecules and permeation enhancers to the intestinal mucosa. J Control Release. 2011;149(1):81–8.
2. Dünnhaupt S, Barthelmes J, Iqbal J, Perera G, Thurner CC, Friedl H, *et al*. *In vivo* evaluation of an oral drug delivery system for peptides based on S-protected thiolated chitosan. J Control Release. 2012;160(3):477–85.
3. Pillay V, Hibbins AR, Choonara YE, du Toit LC, Kumar P, Ndesendo VMK. Orally administered therapeutic peptide delivery: enhanced absorption through the small intestine using permeation enhancers. Int J Pept Res Ther. 2012;18(3):259–80.
4. Amidi M, Mastrobattista E, Jiskoot W, Hennink WE. Chitsan-based delivery systems for protein therapeutics and antigens. Adv Drug Deliv Rev. 2010;62(1):59–82.
5. Breitenbach J. Melt extrusion: from process to drug delivery technology. Euro J Pharm Biopharm. 2002;54(2):107–17.
6. Bernkop-Schnürch A, Paikl C, Valenta C. Novel bioadhesive chitosan-EDTA conjugate protects leucine enkephalin from degradation by aminopeptidase N. Pharmaceut Res. 1997;14(7):917–22.
7. Peppas NA, Kavimandan NJ. Nanoscale analysis of protein and peptide absorption: insulin absorption using complexation and pH-sensitive hydrogels as delivery vehicles. Eur J Pharm Sci. 2006;29(3–4):183–97.
8. Bravo-Osuna I, Millotti G, Vauthier C, Ponchel G. *In vitro* evaluation of calcium binding apacity of chitosan and thiolated chitosan poly(isobutyl cyanoacrylate) core–shell nanoparticles. Int J Pharm. 2007;338(1–2):284–90.
9. Whitehead K, Mitragotri S. Mechanistic analysis of chemical permeation enhancers for oral delivery. Pharm Res. 2008;25(6):1412–9.
10. Westberg C, Benkestock K, Fatouros A, Svensson M, Sj□str□m B. Hexarelin evaluation of factors influencing oral bioavailability and ways to improve absorption. J Pharm Pharmacol. 2001;53(9):1257–64.
11. Graziano JH. Conceptual and practical advances in the measurement and clinical management of lead toxicity. NeuroToxicology. 1993;14(2–3):219–24.
12. Rudraraju VS, Wyandt CM. Rheological characterization of microcrystalline cellulose/sodiumcarboxymethyl cellulose hydrogels using a controlled stress rheometer: part I. Int J Pharm. 2005;292(1–2):53–61.
13. Zhao GH, Kapur N, Carlin B, Selinger E, Guthrie JT. Characterisation of the interactive properties of microcrystalline cellulose-carboxymethyl cellulose hydrogels. Int J Pharm. 2011;415(1–2):95–101.
14. Prodduturi S, Manek RV, Kolling WM, Stodghil SP, Repka MA. Solid-state stability and characterization of hot-melt extruded poly(ethylene oxide) films. J Pharm Sci. 2005;94(10):2232–45.
15. Murphy DJ, Sankalia MG, Loughlin RG, Donnelly RF, Jenkins MG, Carron PAM. Physical characterization and component release of poly(vinyl alchol)-tetrahydroxyborate hydrogels and their applicability as potential topical drug delivery systems. Int J Pharm. 2012;423(2):326–34.
16. El-Arini SK, Clas S-D. Evaluation of disintegration testing of different fast dissolving tablets using the texture analyzer. Pharm Dev Technol. 2002;7(3):361–71.
17. Khoshmanesh A, Cook PLM, Wood BR. Quantitative determination of polyphosphate in sediments using attenuated total reflectance-Fourier transform infrared (ATR-FTIR) spectroscopy and partial least square regression. Analyst. 2012;137:3704–9.
18. de Sousa FB, Oliveira MF, Lula IS, Sansiviero MTC, Cotés ME, Sinisterra RD. Study of inclusion compound in solution involving tetracycline and β-cyclodextrin by FTIR-ATR. Vib Spectrosc. 2008;46(1):57–62.
19. Lloyd GR, Craig DQM, Smith A. An investigation into the melting behaviour of binary mixes and solid dispersions of paracetamonl and PEG 4000. J Pharm Sci. 1997;86(9):991–6.
20. Qi S, Gryczke A, Belton P, Craig DQM. Characterisation of solid dispersions of paracetamol and Eudragit®E prepared by hot-melt extrusion using thermal microthermal and spectroscopic analysis. Int J Pharm. 2008;354(1–2):158–67.
21. Andrews GP, Abudiak OA, Jones DS. Physicochemical characterization of hot melt extruded bicalutamide-polyvinylpyrrolidone solid dispersion. J Pharm Sci. 2010;99(3):1322–35.
22. Gu L, Strickley RG, Chi L-H, Chowhan ZT. Drug-excipient incompatibility studies of dipeptide angiotension-converting enzyme inhibitor, moexipril hydrochloride: drug powder *vs* wet granulation. Pharm Res. 1990;7(4):379–83.
23. Sanganwar GP, Salthigari S, Babu RJ, Gupta RB. Simultaneous production and co-mixing of microparticles of nevirapine and excipients by supercritical antisolvent method for dissolution enhancement. Euro J Pharm Sci. 2010;31(1–3):164–74.
24. Sarode AL, Sandhu H, Shah N, Malick W, Zia H. Hot melt extrusion (HME) for amorphous solid dispersions: predictive tools for processing and impact of drug–polymer interactions on supersaturation. Euro J Pharm Sci. 2013;48(3):371–84.
25. Ellison CD, Ennis BJ, Hamad ML, Lyon RC. Measuring the distribution of density and tabletting force in pharmaceutical tablets by chemical imaging. J Pharm Biomed Anal. 2008;48(1):1–7.
26. van der Voort Maarschalk K, Zuurman K, Vromans H, Bolhuis GK, Lerk CF. Porosity expansion of tablets as a result of bonding and deformation of particulate solids. Int J Pharm. 1996;140(2):185–93.
27. Bashaiwoldu AB, Podczeck F, Newton JM. Compaction of and drug release from coated pellets of different mechanical properties. Adv Powder Technol. 2011;22(3):340–53.
28. Craig DQM. The mechanisms of drug release from solid dispersions in water-soluble polymers. Int J Pharm. 2002;231(2):131–44.
29. Singhal D, Curatolo W. Drug polymorphism and dosage form design: a practical perspective. Adv Drug Deli Rev. 2004;56(3):335–47.